Final Draft
of the original manuscript:

Yang, L.; Ma, L.; Huang, Y.; Feyerabend, F.; Blawert, C.; Hoeche, D.; Willumeit-Roemer, R.; Zhang, E.; Kainer, K.U.; Hort, N.:

Influence of Dy in solid solution on the degradation behavior of binary Mg-Dy alloys in cell culture medium

In: Materials Science and Engineering C (2017) Elsevier

DOI: 10.1016/j.msec.2017.03.010

Influence of Dy in solid solution on the degradation behaviour of binary Mg-Dy alloys in cell culture medium

Lei Yang [ab]*, Liangong Ma [a], Yuanding Huang [b], Frank Feyerabend [b], Carsten Blawert [b], Daniel Höche [b], Regine Willumeit-Römer [b], Erlin Zhang [a], Karl Ulrich Kainer [b], Norbert Hort [b]*

[a] *Key Lab. for Anisotropy and Texture of Materials, Education Ministry of China, School of Materials Science and Engineering, Northeastern University, Shenyang 110819, China*

[b] *Helmholtz Zentrum Geesthacht, Institute of Materials Research, Max-Planck-Str. 1, D-21502 Geesthacht, Germany*

* Corresponding author.

E-mail address: lyang0522@hotmail.com (Lei Yang), Norbert.hort@hzg.de (Norbert Hort)

Abstract

Rare earth element Dy is one of the promising alloying elements for magnesium alloy as biodegradable implants. To understand the effect of Dy in solid solution on the degradation of Mg-Dy alloys in simulated physiological conditions, the present work studied the microstructure and degradation behaviour of Mg-Dy alloys in cell culture medium. It is found the corrosion resistance enhances with the increase of Dy content in solid solution in Mg. This can be attributed to the formation of a relatively more corrosion resistant Dy-enriched film which decreases the anodic dissolution of Mg.

Keywords: Mg-Dy alloys, Dy distribution, degradation, electrochemical behavior

1 Introduction

Magnesium alloys can be used as a new class of degradable biomaterials for medical applications due to the good biocompatibility and appropriate mechanical properties [1-5]. The major issue is that the degradation rates of Mg alloys are high in the physiological environment, which could cause a premature loss of mechanical integrity of the implants before the tissue healing is completed. Mg-RE (RE=rare

earth) based alloys are an important alloying system for medical applications since they have shown a combination of acceptable biocompatibility, excellent mechanical properties and high corrosion resistance. An extensive investigation has been performed on Mg-RE based alloys for medical applications, such as WE43 [6, 7] (4wt% yttrium, 3wt% RE), Mg-Y [8, 9], Mg-Gd [10-12], Mg-Dy [13-15] and Mg-Nd [16-18] based alloys. Additionally, a bone screw made of Mg-RE alloy, with a composition similar to WE43 alloy, has already received the CE (European Conformity) mark and was used clinically [19].

Although Mg-RE alloy medical products are commercial available, the role of RE on the degradation of Mg-RE alloy under physiological conditions is still vague. Regarding the role of Mg-RE intermetallics on the corrosion of Mg, it was reported that it causes galvanic corrosion with Mg matrix, accelerating corrosion rates of Mg [20-22]. The role of RE in solid solution in Mg on corrosion is still not clear. Yao et al. [23] showed that Y in supersaturated Mg-Y alloys improved the passivation ability of the surface of alloys, resulting in increased pitting potential in NaCl solution. However, Zhao et al. investigated the corrosion behavior of RE metals (Dy, Gd, Nd and Y) in NaCl solution and they found these RE metals have weak ability for passivation [24]. Schlüter et al. compared the corrosion performance of pure Mg and sputter deposited Mg-Gd and Mg-Y alloys, displaying that both of Y and Gd have little effects on corrosion of Mg [25]. Therefore, further study is needed to fully clarify the role of RE in solid solution on the corrosion of Mg alloys.

Among all RE elements, Dy is one of the best tolerated elements based on *in vitro* study [26]. It has a large flexibility in adjusting the mechanical and corrosion properties of Mg-RE alloys due to its high solid solubility in Mg (maximum 25.3 wt%) [27]. Previous work showed that Mg-Dy alloys are very promising for medical applications [13-15]. The aim of present work is to clarify the role of Dy on the

degradation of binary Mg-Dy alloys in cell culture medium.

2 Experimental procedures

2.1 Materials preparation

Permanent mould direct chill casting was used to prepare Mg-xDy (x = 5, 10, 15 and 20 wt%) alloys. High-purity Mg (99.94%) was molten in a mild steel crucible under a protective atmosphere (Ar + 2% SF_6). Pure Dy (10, 15 and 20 wt%) was added at a melt temperature of 720 °C. Then the melt was stirred for 30 min at 200 rpm and then poured into a mould preheated to 500 ^{o}C. The filled mould was held at 670 ^{o}C for 30 min under the protective gas and then it was slowly quenched in continuous cooling water. The size of ingot was 20 cm×12 cm×6 cm. Solution treatment (T4) was carried out at 520°C for 24h followed by water quenching. All specimens were taken from the similar location in the ingots. The chemical compositions of the alloys, as listed in Table 1, were analyzed using X-ray fluorescence (XRF) analyzer (Bruker AXS S4 Explorer, Germany) for Dy and Ni, and using spark optical emission spectroscopy (Spectrolab M9 Kleve, Germany) for Fe and Cu. Regarding the measurement of impurities with spark optical emission spectroscopy, the content of Ni could not be determined due to interference of strong Dy peaks. Therefore, the Ni content was determined by XRF. The content of impurities is very low and similar in the Mg-Dy alloys studied. Thus, its effect on the alloys is not taken into account in this study.

2.2 Microstructure

Specimens for microstructural characterization were ground using silicon carbide emery paper up to 2500 grit, and then mechanically polished with 0.05 μm colloidal silica (OPS). The polished specimens were etched in a solution with 4 g picric acid, 5

ml acetic acid, 10 ml distilled water and 100 ml ethanol. The optical microstructure was characterized using a light microscope (Reichert-Jung MeF3, Germany). A Zeiss Ultra 55 (Carl Zeiss GmbH, Oberkochen, Germany) scanning electron microscope (SEM) instrument, equipped with energy dispersive X-ray spectroscopy (EDS) was employed to observe the microstructure and morphologies of corrosion layer and corroded surfaces. The Dy distribution in the alloys was measured using EDS.

2.3 XPS analysis

X-ray induced photoelectron spectroscopy (XPS) measurements were carried out on a Kratos Axis Ultra DLD (Kratos Analytical Ltd., Manchester, UK) attached with a 15 KV X-ray gun using monochromatic Al Kα radiation. The specimens of Mg-10Dy alloy and pure Dy metal were immersed in the cell culture medium (CCM) under cell culture conditions (37°C, 21% O_2, 5% CO_2, 95% rH) for 24 h and 1 h, respectively. Specimens were cleaned with distilled water and dried in vacuum. The XPS measurements were conducted on an area of 700 μm × 300 μm with pass energy of 40 eV at the regions of measurements and 160 eV for survey scans. As a result of the nonconductive nature of the corrosion products, a charge neutralizer was used to correct the chemical shifts caused by charging. Argon ions (4000 eV), with an etching rate of about 40 nm/min, were used to etch the specimens in order to investigate the composition of corrosion layer at different depth. Curve fitting of the spectra was conducted with Casa 2.3.15 software (Casa Software Ltd., Teighnmouth, Devon, UK, 2003). Element binding energy database used is the NIST Standard Reference Database 20, Version 3.5.

2.4 Degradation test

For the degradation tests in CCM under cell culture conditions, the specimens,

with a diameter of 10.0 mm and a height of 1.5 mm, were prepared by grinding each side with 2400 grid emery paper and degreasing the surfaces with ethanol prior to corrosion tests. The specimens were sterilized in 70% ethanol for 15 min before the start of tests. To observe the effect of Dy distribution on the formation of corrosion layer, the specimens were immersed in CCM under cell culture condition for 1 and 3 days and then cleaned with deionized water and dried in air. To observe the effect of Dy distribution on the morphologies of corroded surfaces of Mg-Dy alloys, the specimens were immersed in CCM under cell culture condition for 14 days, and then the corrosion products were removed by immersing the corroded specimens in chromic acid (180 g/l) for 20 min at room temperature. The morphologies of corrosion layer and surfaces of specimens after the removal of corrosion products were observed using SEM. Thickness of corrosion layer (immersion for 3 days) for solid solution heat treated specimens was measured using optical microscope observing the cross section of corrosion layer. Six images were taken randomly for each specimen, and the thickness of corrosion layer at five regions was measured for each image.

Electrochemical tests were carried out using a Gill AC potentiostat / frequency response analyser system. A typical three electrode cell was used, equipped with a Ag/AgCl electrode (with 3mol/l KCl) as a reference, a platinum mesh as a counter electrode and a specimen with 0.5 cm^2 surface area as a working electrode. The electrochemical tests were conducted in 300 ml cell culture medium (CCM) at atmospheric conditions without stirring. The CCM is consisted of Dulbecco's modified Eagle medium (DMEM; Life Technologies, Darmstadt, Germany) and 10% fetal bovine serum (PAA Laboratories, Linz, Austria). The composition of the DMEM can be found elsewhere [15]. Electrochemical impedance spectroscopy (EIS) studies were performed at open circuit potential with an AC amplitude of 10mV over the

frequency range of 30,000–0.01 Hz. EIS was measured at different durations to understand the degradation phenomena. Potentiodynamic polarisation tests were performed at a scan rate of 1 mVs^{-1}.

3 Results and discussion

3.1 Microstructure and corrosion behaviour

Figure 1 shows the optical microstructure of Mg-Dy alloys. It is comprised of Mg matrix, region of Dy segregation and $Mg_{24}Dy_5$ second phase (at the centre of region of Dy segregation). The Dy content analyzed by EDS, at the matrix is about half of the Dy content in Mg-Dy alloys, and at the area of segregation is in the range of 19-28wt% in Mg-Dy alloys, which can be found elsewhere [13]. In order to understand the influence of the distribution of Dy on the corrosion behavior of Mg-Dy alloys, the morphologies of corrosion layer after immersion for 1 day in CCM were observed. For all the Mg-Dy alloys, the morphologies of corrosion layer are nonuniform, which are consisted of dark and bright corroded areas. The morphologies of corrosion layer of Mg-10Dy and Mg-20Dy alloys are presented here as the representatives (Figure 2). For Mg-Dy alloys, the Mg matrix was corroded significantly, which shows dark color in optical images (Figure 2 a and b) and shows bright color in SEM images (Figure 2 c and d). However, the region of Dy segregation was corroded only slightly, which presents bright color in optical images (Figure 2 a and b) and dark color in SEM images (Figure 2 c and d). Further EDS analysis confirms the different compositions in these different areas. In the dark areas, large amount of Mg (94.26 at.%) and little amount of O (0.81at.%) were detected (point A), indicating only marginal corrosion occurs in these areas. In the bright areas, 16.79 at.% O and 57.44 at.% Mg were detected (point B). This implies some corrosion has occurred in these areas and the corrosion film has formed. With the increase of Dy, the corroded areas are reduced

due to the increase of region of Dy segregation. This indicates that the segregation of Dy improves the corrosion resistance and reduces the formation of corrosion products on these areas.

To further confirm the influences of Dy distribution in Mg on the corrosion behavior of Mg, Figure 3 shows the morphologies of corroded surfaces of as-cast Mg-Dy alloys after immersion for 14 days in CCM and removal of the corrosion products. As the results are similar for all the alloys, only the results of Mg-10Dy and Mg-20Dy alloys are presented here as the representatives. As shown in Figure 3, corrosion follows the cast dendritic structure. The EDS analysis, as indicated on the images, reveals that the content of Dy at the prominent area is very close to that in the region of Dy segregation [13]. This indicates that the regions with Dy segregation are more corrosion resistant than the Mg matrix with less Dy content. Similar results were reported by Davenport et al., which monitored 3D evolution morphology for a corroded WE43 (Mg-4Y-3Nd-0.5Zr, wt%) alloy using synchrotron X-Ray micro-tomography. They found that the Y-rich regions of the matrix slowed the propagation of corrosion [28].

Figure 4 shows the morphologies of corroded surfaces of T4 treated Mg-10Dy and Mg-20Dy alloys after immersion in CCM for 14 days and removal of the corrosion products. Since similar morphologies of corroded surfaces were observed for Mg-5Dy and Mg-15Dy alloys, it is not shown here. Compared with the morphologies of corroded surfaces of as-cast Mg-Dy alloys, the dendritic morphology disappeared. This is due to the homogeneous distribution of Dy in the alloys, leading to the uniform degradation of Mg-Dy alloys. The corrosion occurred on Mg-10Dy is more serious than that on Mg-20Dy. For Mg-10Dy, some round plain areas were formed due to the formation of hydrogen bubbles at these areas. For Mg-20Dy, the scratches still can be seen, indicating minor corrosion occurred on the surface. The EDS analysis

shows all the area has the similar Dy content to that of the Dy content in the alloys.

Figure 5 shows the morphologies of corrosion layers of Mg-Dy alloys with T4 treatment after immersion in CCM for 3 days. The cracks on the surfaces were formed due to dehydration of the corrosion layer. The corrosion layers are uniform on the surfaces of Mg-5Dy and Mg-10Dy alloys. For Mg-15Dy alloy, some part of the corrosion layer is thick and some part is thin. The pitting corrosion has even occurred on Mg-20Dy alloy as indicated by arrow F (Figure 5d). To study the distribution of alloying element Dy in the corrosion layer, the composition of the corrosion layer was analyzed by EDS (Table 2). The enrichment of Dy in the corrosion layer is found for all alloys. The Dy content increases in the corrosion layer with the increase of Dy from 5 to 15 wt. % in the alloys (point (A, B, C)). For Mg-20Dy alloy, the Dy content is supposed to be higher in the corrosion layer than that of Mg-15Dy. However, due to the thin corrosion layer on Mg-20Dy alloy, some of the EDS signal derives from the substrate. As a result, large amount of Mg (51.1 and 78.3 at.%) was detected at the points D and E, and the detected Dy content is not as high as expected.

The morphologies of cross-section corrosion layers after immersion for 3 days are shown in Figure 6. It displays that the thickness of corrosion layer reduces with the increase of Dy content. As listed in Table 3, the thickness of the corrosion layer decreases from around 14.6 μm to 4.4 μm when Dy content increases from 5 to 15wt%. Moreover, it is below 2 μm at the most areas except that of pitting corrosion for the Mg-20Dy alloy (Figure 6d). The reduction in layer thickness indicates the corrosion resistance is improved with increase of Dy accumulation in the corrosion layer regardless of the pitting corrosion.

To investigate the distribution of corrosion products of alloying element Dy, XPS analysis was performed (Figure 7). First, XPS analysis was carried out for Mg-10Dy alloy after immersion in CCM for 24 hours and etched with argon ion sputtering

for 500 s (Figure 7 a). The Dy peak can be fitted to two peaks. The higher one (at 306 eV) corresponds to Dy_2O_3. It is not clear the species to which the lower peak corresponds since the database for the binding energy of Dy peaks is not complete. In order to further clarify the distribution of corrosion products of Dy in CCM, XPS analysis was also conducted on pure Dy specimen after immersion in CCM for 1 hour. As presented in Figure 7 b, two main peaks are observed for O_{1s}, corresponding to $Dy(OH)_3$ (at 531.2 eV) and Dy_2O_3 (at 528.8 eV), respectively. With increasing etching time, the intensity of $Dy(OH)_3$ peak decreases. This indicates that the amount of $Dy(OH)_3$ decreases from the outer corrosion layer to the inner corrosion layer. Dy metal is quite active, and has a similar standard electrode potential (-2.35V) to Mg (-2.37V) [29]. It was reported that Dy could be enriched in the corrosion layer existing as corrosion products of Dy_2O_3 and $Dy(OH)_3$ [15]. In the present work, it is further found that $Dy(OH)_3$ is mainly distributed at the outer corrosion layer and Dy_2O_3 is mainly at the inner corrosion layer. It should be pointed out that RE are reported to accumulate in bones in human body, which could replace Ca in hydroxyapatite [30, 31]. Hence, a small amount of Dy phosphate in the degradation products could be formed. However, the XPS database does not include the information of Dy phosphate. Further investigation is needed.

3.2 Electrochemical behaviour

EIS tests were employed to understand the corrosion process of Mg-Dy alloys (Figure 8). For Mg-5Dy, Mg-10Dy and Mg-15Dy alloys, the capacitive loops are obtained at different immersion time. Their diameter increases with the increase in immersion time up to 48 h. For Mg-20Dy alloy, up to immersion for 12 h the Nyquist plots only show capacitive loops. With further immersion, the inductive loop is

obtained. It was reported that the inductive loop formed was due to the breakdown of corrosion film and formation of pitting corrosion [32]. In order to compare the corrosion resistance of Mg-Dy alloys after immersion in CCM for different time, the polarization resistance (R_p) was extracted from the Nyquist plots by subtracting the corrosion resistance at 100 kHz from the corrosion resistance at 0.01Hz (in theory frequency close to zero). For Mg-(5-15)Dy alloys, the R_p increases with the increase of immersion time. However, for Mg-20Dy alloys, the Rp increases rapidly with the increase in immersion time up to 12 hours. After 12 hours the film broke down then it decreases. Generally, before the breakdown of corrosion film, the R_p increases faster for Mg-Dy alloys with higher Dy content. It is not clear why the breakdown of corrosion film on Mg-20Dy alloy occurred. Since some of the $Mg_{24}Dy_5$ phase in T4 treated Mg-20Dy alloy is undissolved as revealed elsewhere [13, 14], the breakdown of corrosion film on Mg-20Dy alloy is possibly due to the galvanic corrosion between the Mg matrix and the undissolved $Mg_{24}Dy_5$ phase.

To evaluate the effect of Dy in solid solution on the electrochemical reaction kinetics of Mg-Dy alloys, the potential dynamic polarization curves of Mg-Dy alloys after immersion in CCM for 48 hours at room temperature were measured as presented in Figure 10. The cathodic reaction kinetics is similar for Mg-(5, 10, 15)Dy alloys. The anodic reaction kinetics reduces with the increase of Dy content up to 15 wt% in alloys. As a result, the corrosion current density decreases and the corrosion potential increases with the increase of Dy content up to 15 wt% (Table 4). For Mg-20Dy alloys, the cathodic reaction kinetics is much higher than that of Mg-(5-15)Dy alloys. This is possibly due to the undissolved $Mg_{24}Dy_5$ intermetallics [14] which support higher cathodic reaction rate. Furthermore, the breakdown of degradation film on Mg-20Dy alloy could be another reason. It is reported that for Mg alloys once the corrosion film broke down, impurities, second phase particles and alloying

elements could accumulate at the corroded area, which significantly enhances the cathodic reaction kinetics [33-35]. The decreased anodic reaction kinetics was also observed with increasing the yttrium (Y) content in Mg-Y model alloys with no second phase particles, prepared through magnetron sputtering [23, 36]. This was attributed to the Y-enriched corrosion layer. The enhanced passivity for the corrosion film is mainly due to the incorporation of Y_2O_3 rather than $Y(OH)_3$ in it [23].

4 Conclusion

The microstructure and degradation behaviour of Mg-Dy alloys in cell culture medium were studied. The following conclusions can be made.

1. For as-cast Mg-Dy alloys, the regions with Dy segregation are more corrosion resistant than Mg matrix with relatively less Dy content in cell culture medium. For solution heat treated Mg-Dy alloys, corrosion resistance increases with increasing Dy content before the breakdown of degradation film.
2. Dy released from the degradation of Mg-Dy alloys in CCM goes into the corrosion layer to form Dy_2O_3 and $Dy(OH)_3$, leading to the improvement of corrosion resistance for Mg-Dy alloys.
3. Dy in solid solution does not alter the cathodic reaction kinetics of Mg-Dy alloys, but it decreases the anodic reaction kinetics.

Acknowledgement

The authors would like to thank Mrs. G. Salamon for technical assistance. Financial support from the National Nature Science Foundation of China (No. 51601036) is also gratefully acknowledged.

References

[1] M.P. Staiger, A.M. Pietak, J. Huadmai, G. Dias, Magnesium and its alloys as orthopedic biomaterials: A review, Biomaterials, 27 (2006) 1728-1734.
[2] R.C. Zeng, W. Dietzel, F. Witte, N. Hort, C. Blawert, Progress and challenge for magnesium alloys as biomaterials, Adv. Eng. Mater., 10 (2008) B3-B14.
[3] F. Witte, N. Hort, C. Vogt, S. Cohen, K.U. Kainer, R. Willumeit, F. Feyerabend, Degradable biomaterials based on magnesium corrosion, Current Opinion in Solid State & Materials Science, 12 (2008) 63-72.
[4] X. Gu, Y.F. Zheng, A review on magnesium alloys as biodegradable materials Front. Mater. Sci. China, 4 (2010) 111–115.
[5] S. Agarwal, J. Curtin, B. Duffy, S. Jaiswal, Biodegradable magnesium alloys for orthopaedic applications: A review on corrosion, biocompatibility and surface modifications, Materials Science and Engineering: C.
[6] F. Witte, V. Kaese, H. Haferkamp, E. Switzer, A. Meyer-Lindenberg, C.J. Wirth, H. Windhagen, In vivo corrosion of four magnesium alloys and the associated bone response, Biomaterials, 26 (2005) 3557-3563.
[7] F. Witte, J. Fischer, J. Nellesen, H.A. Crostack, V. Kaese, A. Pisch, F. Beckmann, H. Windhagen, In vitro and in vivo corrosion measurements of magnesium alloys, Biomaterials, 27 (2006) 1013-1018.
[8] A.C. Hanzi, P. Gunde, M. Schinhammer, P.J. Uggowitzer, On the biodegradation performance of an Mg-Y-RE alloy with various surface conditions in simulated body fluid, Acta Biomater., 5 (2009) 162-171.
[9] A.C. Hanzi, I. Gerber, M. Schinhammer, J.F. Loffler, P.J. Uggowitzer, On the in vitro and in vivo degradation performance and biological response of new biodegradable Mg-Y-Zn alloys, Acta Biomater., 6 (2010) 1824-1833.
[10] N. Hort, Y. Huang, D. Fechner, M. Stomer, C. Blawert, F. Witte, C. Vogt, H. Drüker, R. Willumeit, K.U. Kainer, F. Feyerabend, Magnesium alloys as implant materials - Principles of property design for Mg-RE alloys, Acta Biomater., 6 (2010) 1714-1725.
[11] A. Myrissa, N.A. Agha, Y. Lu, E. Martinelli, J. Eichler, G. Szakács, C. Kleinhans, R. Willumeit-Römer, U. Schäfer, A.-M. Weinberg, In vitro and in vivo comparison of binary Mg alloys and pure Mg, Materials Science and Engineering: C, 61 (2016) 865-874.
[12] J. Zhang, Z. Kang, F. Wang, Mechanical properties and biocorrosion resistance of the Mg-Gd-Nd-Zn-Zr alloy processed by equal channel angular pressing, Materials Science and Engineering: C, 68 (2016) 194-197.
[13] L. Yang, Y.D. Huang, Q.M. Peng, F. Feyerabend, K.U. Kainer, R. Willumeit, N. Hort, Mechanical and corrosion properties of binary Mg-Dy alloys for medical applications, Mater Sci Eng B-Adv, 176 (2011) 1827-1834.
[14] L. Yang, Y. Huang, F. Feyerabend, R. Willumeit, K.U. Kainer, N. Hort, Influence of ageing treatment on microstructure, mechanical and bio-corrosion properties of Mg–Dy alloys, Journal of the mechanical behavior of biomedical materials, 13 (2012) 36-44.
[15] L. Yang, N. Hort, D. Laipple, D. Höche, Y. Huang, K.U. Kainer, R. Willumeit, F. Feyerabend, Element distribution in the corrosion layer and cytotoxicity of alloy Mg–10Dy during in vitro biodegradation, Acta Biomater., 9 (2013) 8475-8487.
[16] X. Zhang, G. Yuan, L. Mao, J. Niu, P. Fu, W. Ding, Effects of extrusion and heat treatment on the mechanical properties and biocorrosion behaviors of a Mg–Nd–Zn–Zr alloy, Journal of the Mechanical Behavior of Biomedical Materials, 7 (2012) 77-86.
[17] Y.P. Wang, Z.J. Zhu, Y.H. He, Y. Jiang, J. Zhang, J.L. Niu, L. Mao, G.Y. Yuan, In vivo degradation behavior and biocompatibility of Mg-Nd-Zn-Zr alloy at early stage, International Journal of Molecular Medicine, 29 (2012) 178-184.
[18] O. Hakimi, E. Aghion, J. Goldman, Improved stress corrosion cracking resistance of a novel biodegradable EW62 magnesium alloy by rapid solidification, in simulated electrolytes, Materials

Science and Engineering: C, 51 (2015) 226-232.
[19] H. Hermawan, D. Dubé, D. Mantovani, Developments in metallic biodegradable stents, Acta Biomater., 6 (2010) 1693-1697.
[20] N. Birbilis, M.A. Easton, A.D. Sudholz, S.M. Zhu, M.A. Gibson, On the corrosion of binary magnesium-rare earth alloys, Corros. Sci., 51 (2009) 683-689.
[21] A. Sudholz, K. Gusieva, X. Chen, B. Muddle, M. Gibson, N. Birbilis, Electrochemical behaviour and corrosion of Mg–Y alloys, Corros. Sci., 53 (2011) 2277-2282.
[22] M. Liu, P. Schmutz, P.J. Uggowitzer, G. Song, A. Atrens, The influence of yttrium (Y) on the corrosion of Mg-Y binary alloys, Corros. Sci., 52 (2010) 3687-3701.
[23] H. Yao, Y. Li, A. Wee, Passivity behavior of melt-spun Mg–Y alloys, Electrochim. Acta, 48 (2003) 4197-4204.
[24] X. Zhao, L.-l. Shi, J. Xu, A comparison of corrosion behavior in saline environment: rare earth metals (Y, Nd, Gd, Dy) for alloying of biodegradable magnesium alloys, Journal of Materials Science & Technology, 29 (2013) 781-787.
[25] K. Schlüter, Z. Shi, C. Zamponi, F. Cao, E. Quandt, A. Atrens, Corrosion performance and mechanical properties of sputter-deposited MgY and MgGd alloys, Corros. Sci., 78 (2014) 43-54.
[26] F. Feyerabend, J. Fischer, J. Holtz, F. Witte, R. Willumeit, H. Drückere, C. Vogt, N. Hort, Evaluation of short-term effects of rare earth and other elements used in magnesium alloys on primary cells and cell lines, Acta Biomater., 6 (2010) 1834-1842.
[27] A.A. Nayeb-Hashemi, J.B. Clark, Phase Diagram of Binary Magnesium Alloys, ASM International, Metal Park, OH, USA, 1988.
[28] A.J. Davenport, C. Padovani, B.J. Connolly, N.P. Stevens, T.A. Beale, A. Groso, M. Stampanoni, Synchrotron X-ray microtomography study of the role of Y in corrosion of magnesium alloy WE43, Electrochem. Solid-State Lett., 10 (2007) C5-C8. [29] G. Milazzo, S. Caroli, R.D. Braun, Tables of standard electrode potentials, J. Electrochem. Soc., 125 (1978) 261C-261C.
[30] V. Zaichick, Chemical elements of human bone tissue investigated by nuclear analytical and related methods, Biol. Trace Elem. Res., 153 (2013) 84-99.
[31] S. Zaichick, V. Zaichick, V. Karandashev, S. Nosenko, Accumulation of rare earth elements in human bone within the lifespan, Metallomics, 3 (2011) 186-194.
[32] F. Cao, Z. Shi, J. Hofstetter, P.J. Uggowitzer, G. Song, M. Liu, A. Atrens, Corrosion of ultra-high-purity Mg in 3.5% NaCl solution saturated with Mg $(OH)_2$, Corros. Sci., 75 (2013) 78-99.
[33] S. Thomas, N.V. Medhekar, G.S. Frankel, N. Birbilis, Corrosion mechanism and hydrogen evolution on Mg, Curr. Opin. Solid State Mater. Sci., 19 (2015) 85-94.
[34] M. Taheri, J.R. Kish, N. Birbilis, M. Danaie, E.A. McNally, J.R. McDermid, Towards a Physical Description for the Origin of Enhanced Catalytic Activity of Corroding Magnesium Surfaces, Electrochim. Acta, 116 (2014) 396-403.
[35] G. Frankel, A. Samaniego, N. Birbilis, Evolution of hydrogen at dissolving magnesium surfaces, Corros. Sci., 70 (2013) 104-111.
[36] P. Miller, B. Shaw, R. Wendt, W. Moshier, Assessing the corrosion resistance of nonequilibrium magnesium-yttrium alloys, Corrosion, 51 (1995) 922-931.

Figure

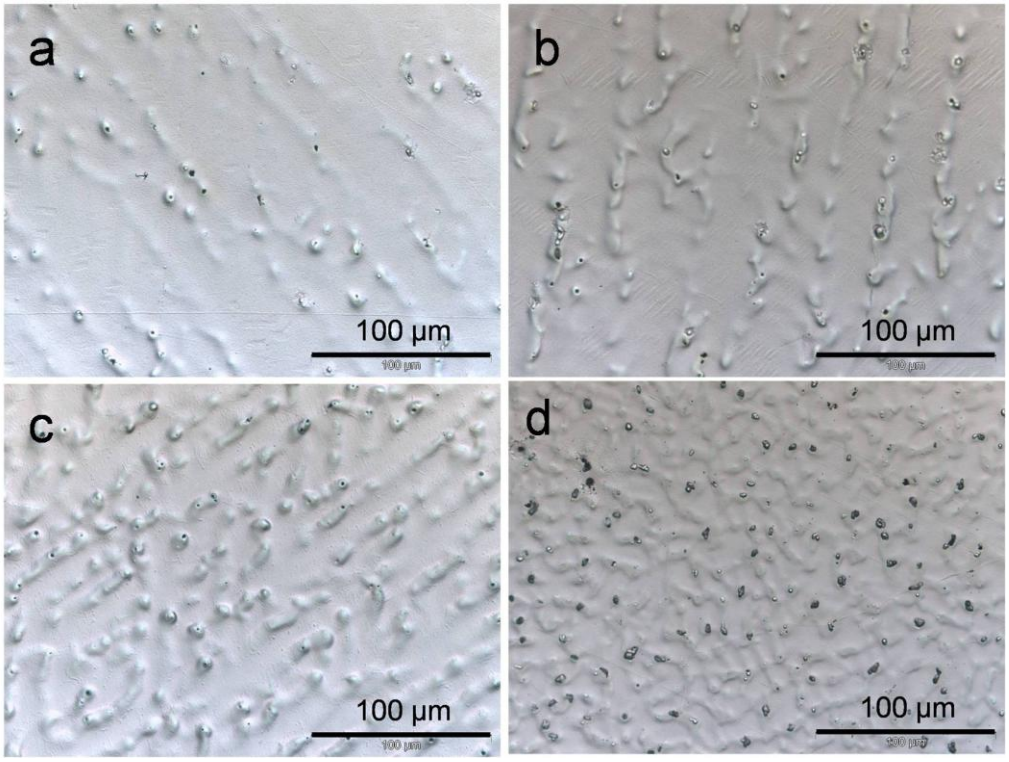

Figure 1. Optical microstructures of Mg-Dy alloys: (a) Mg-5Dy; (b) Mg-10Dy; (c) Mg-15Dy; (d) Mg-20Dy.

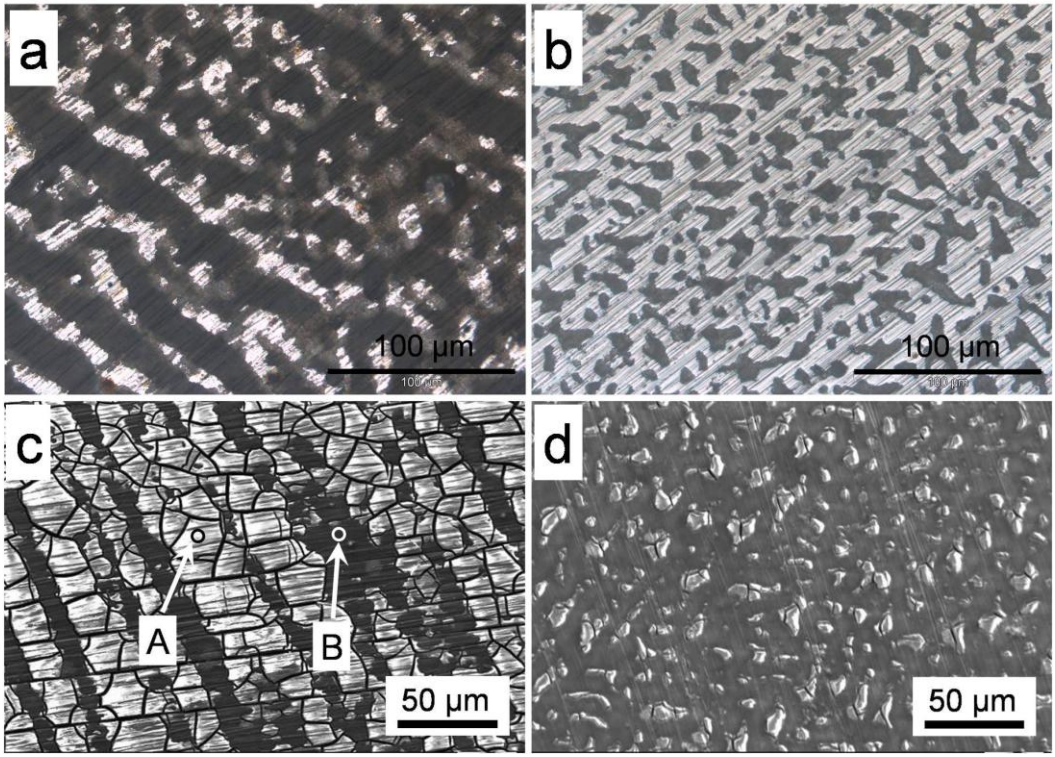

Figure 2. Corrosion morphologies after 1 day immersion in CCM under cell culture conditions：(a) Optical image of Mg-10Dy; (b) Optical image of Mg-20Dy; (c) SEM image of Mg-10Dy; (d) SEM image of Mg-20Dy.

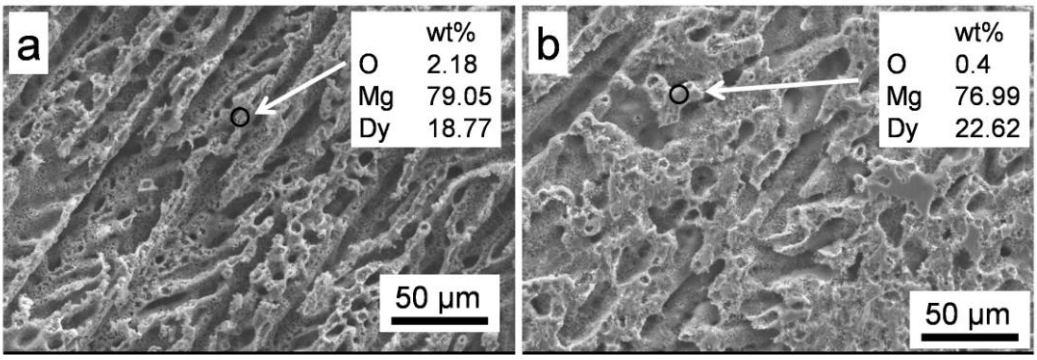

Figure 3. Corrosion morphologies of as-cast Mg-10Dy and Mg-20Dy alloys after immersion for 14 days in CCM and removal of the corrosion products.

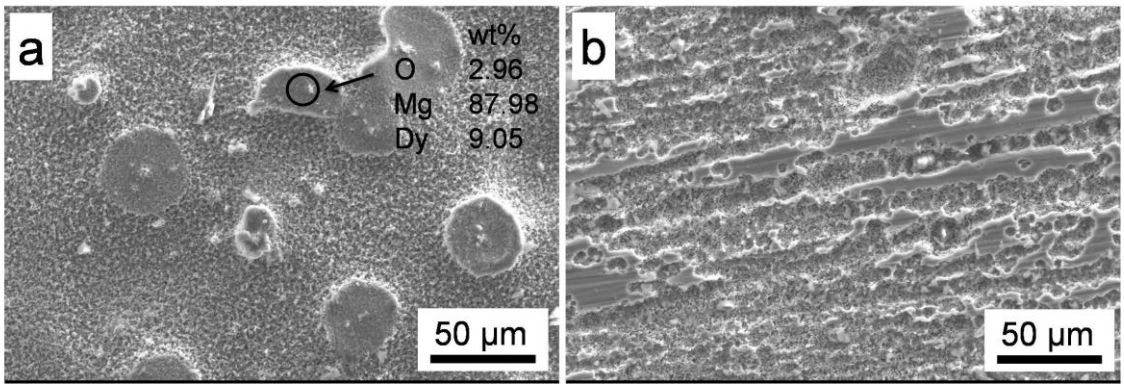

Figure 4. Corrosion morphologies of T4 treated Mg-10Dy and Mg-20Dy alloys after immersion in CCM for 14 days and removal of the corrosion products.

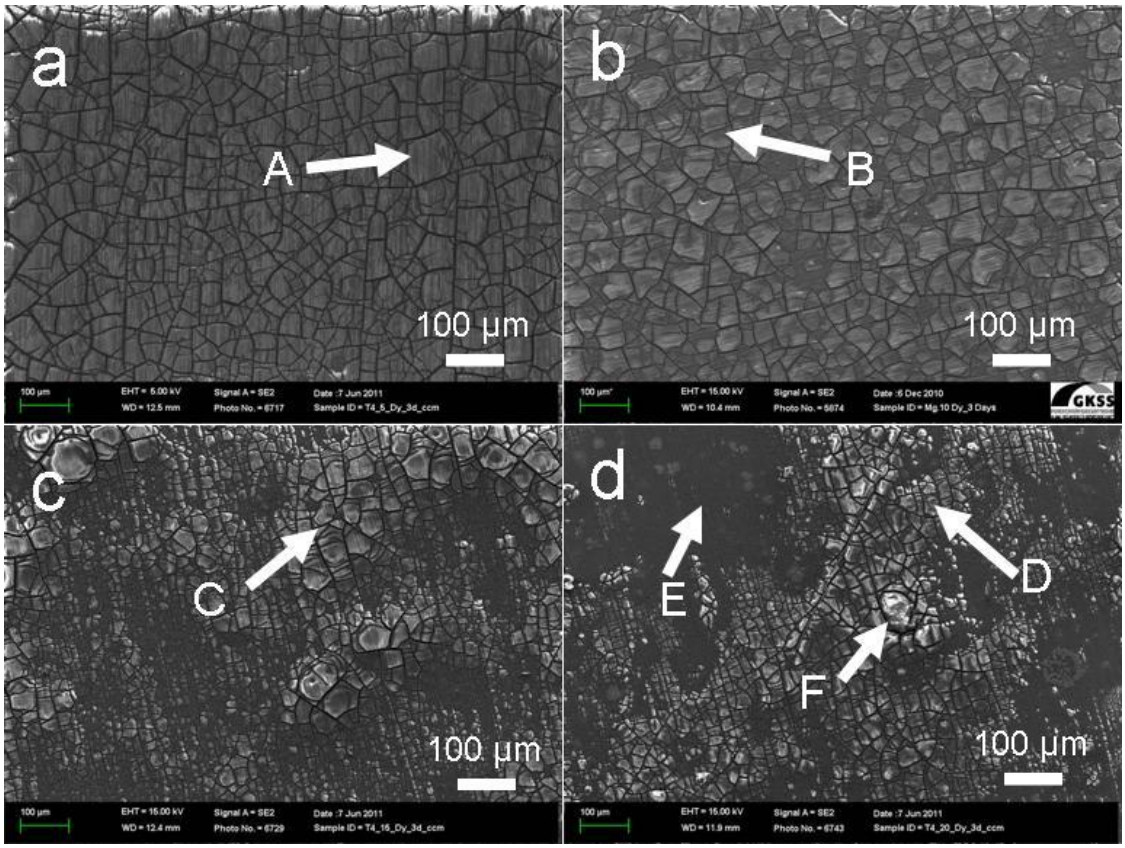

Figure 5. Corrosion morphologies of Mg-Dy alloys with T4 treatment after immersion in CCM for 3 days under cell culture conditions: (a) Mg-5Dy; (b) Mg-10Dy; (c) Mg-15Dy; (d) Mg-20Dy

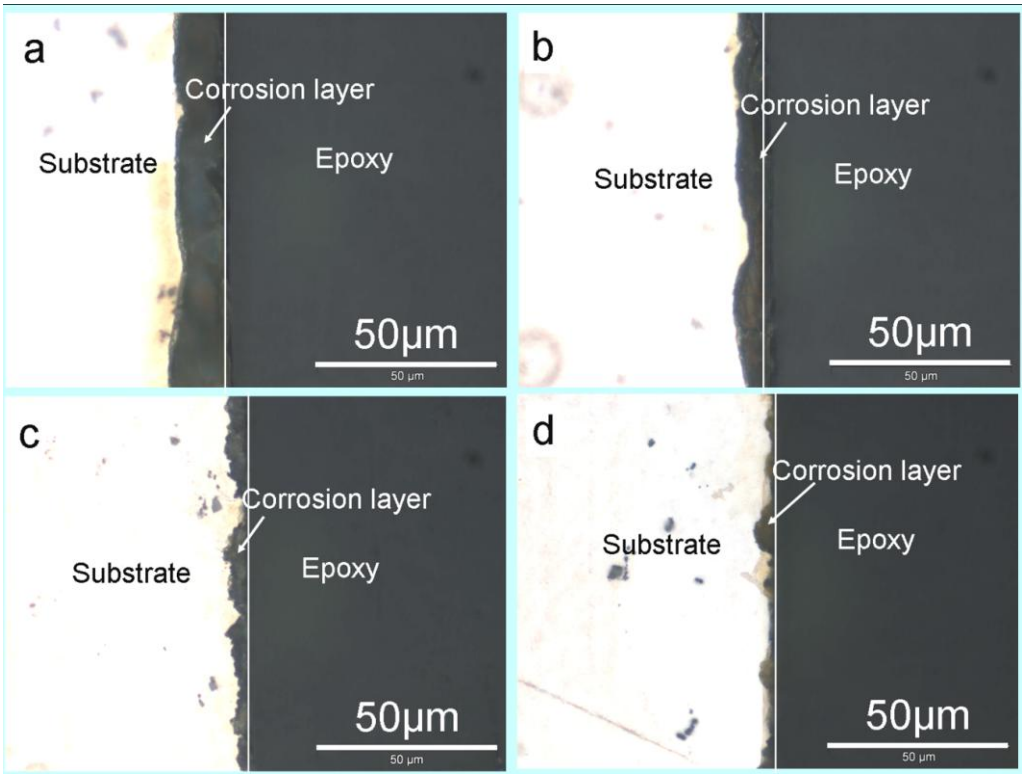

Figure 6. Morphologies of cross sections for Mg-Dy alloys with T4 treatment after immersion in CCM 3 days under cell culture conditions: (a) Mg-5Dy; (b) Mg-10Dy; (c) Mg-15Dy; (d) Mg-20Dy.

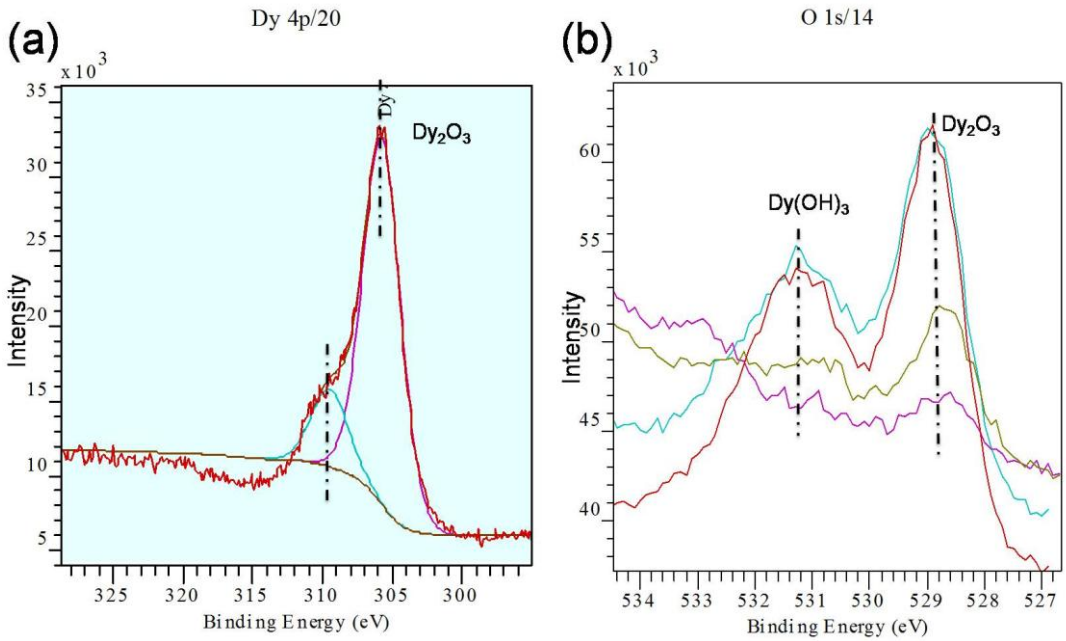

Figure 7. Peaks of binding energy obtained by XPS analysis: (a) Dy peaks of Mg-10Dy specimen after immersion in CCM for 24 hours and etched with argon ion sputtering for 500 s; (b) O peaks of pure Dy specimen after immersion in CCM for 1 hours and etched with argon ion sputtering for different times.

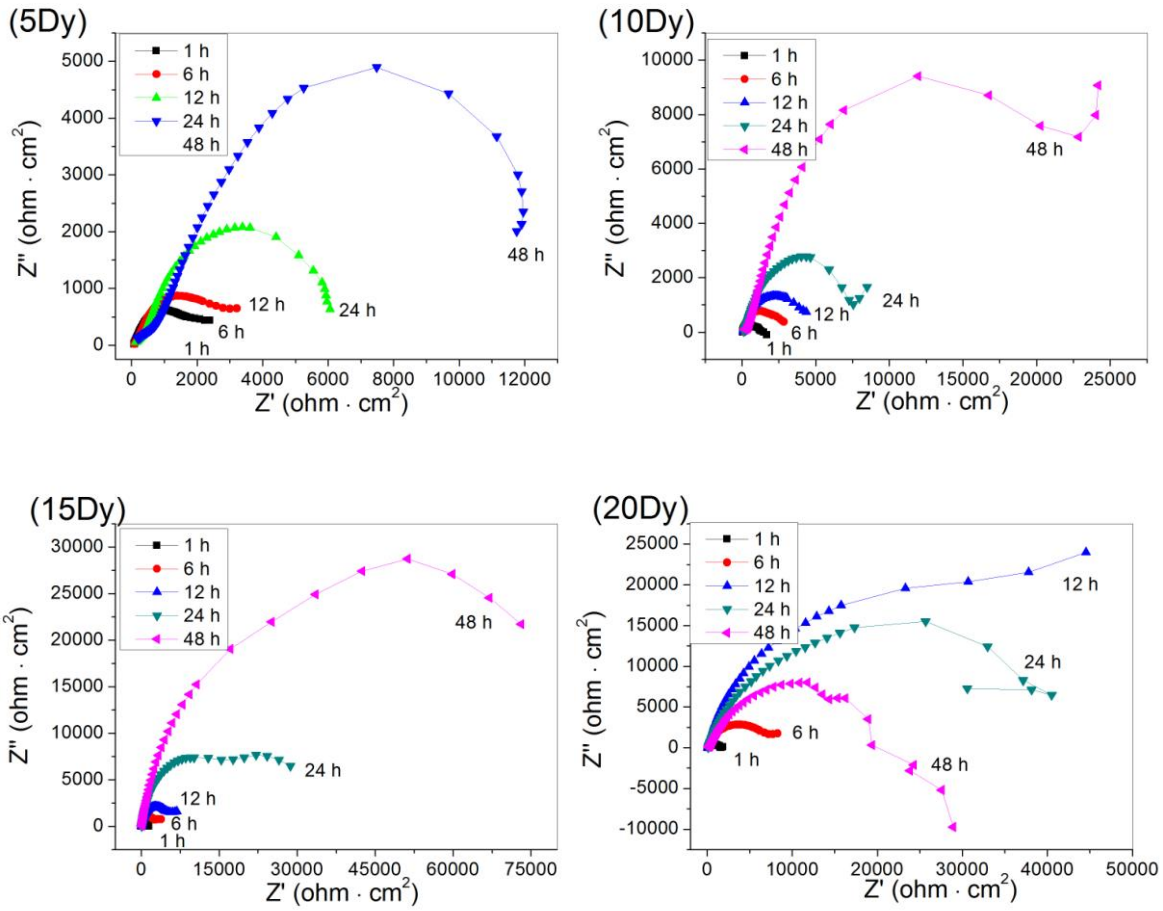

Figure 8. Electrochemical impedance spectrum (Nyquist plots) of Mg-Dy alloys in CCM at room temperature.

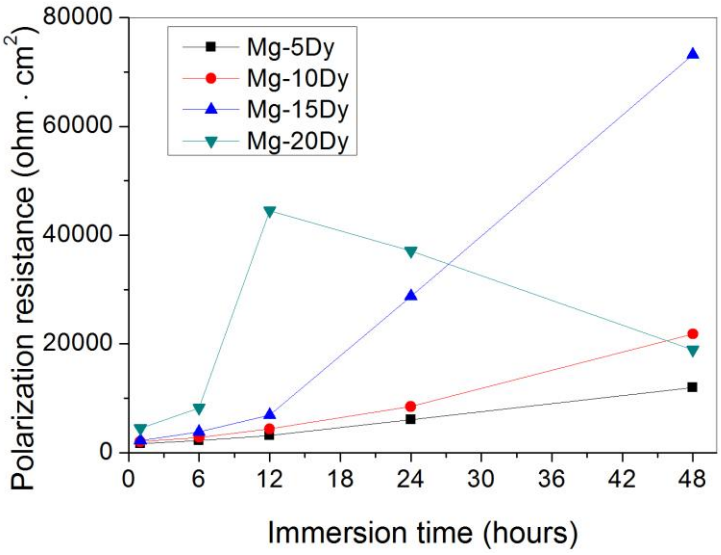

Figure 9. Polarization resistance of Mg-Dy alloys extracted from the Nyquist plots.

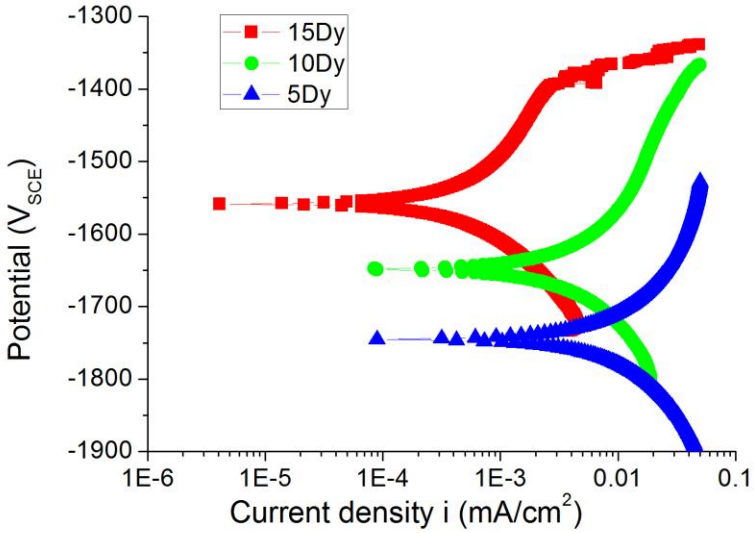

Figure 10. Potential dynamic polarization curves of T4 treated Mg-Dy alloys after immersion in CCM for 48 hours at room temperature.

Table

Table 1: Chemical compositions of experimental alloys (wt.%).

Alloys	Dy	Fe	Ni	Cu	Mg
Mg-5Dy	4.500	0.004	<0.004	0.070	Balance
Mg-10Dy	9.200	0.005	<0.004	0.007	Balance
Mg-15Dy	13.000	0.007	<0.004	0.008	Balance
Mg-20Dy	18.600	0.009	<0.004	0.010	Balance

Table 2. Compositions analyzed by EDS for the points shown in the corrosion layers (Figure 5) (at.%).

	C	O	Mg	P	Ca	Dy
Point A	3.77	43.37	25.71	10.89	8.81	7.45
Point B	3.75	32.04	24.91	8.18	10.36	17.67
Point C	3.70	27.25	20.49	9.25	6.89	32.40
Point D	2.89	19.16	51.10	3.57	3.74	19.54
Point E	0.20	14.53	78.31	2.53	1.16	3.47

Table 3. Thickness of corrosion layer after immersion in CCM for 3 days under cell culture conditions.

Alloys	Mg-5Dy	Mg-10Dy	Mg-15Dy	Mg-20Dy
Layer thickness (μm)	14.6±4.8	9.4±3.3	4.4±1.9	3.1±2.1

Table 4. Corrosion parameters derived from the polarization curves shown in Figure 10.

Alloys	Mg-5Dy	Mg-10Dy	Mg-15Dy
Corrosion potential (V_{SCE})	-1.746	-1.650	-1.554
Corrosion current density (mA/cm^2)	0.011	0.005	0.002